Research Square

Preprints are preliminary reports that have not undergone peer review.
They should not be considered conclusive, used to inform clinical practice,
or referenced by the media as validated information.

Development of Forest Fire Hotspot Identification and Rapid Evaluation Technique for Tropical Landscapes Utilizing Open-access Climatic and Soil Data (FIRE-TROPICS)

Geronimo Allan Jerome G. Acosta

gacosta@psu.palawan.edu.ph

Palawan State University

John Vincent C. Colili

Palawan State University

Rodolfo O. Abalus, Jr.

Palawan State University

Jean V. Malolos

University of the Philippines Diliman

Research Article

Keywords: forest fire susceptibility, machine learning, geospatial analysis, remote sensing

Posted Date: June 16th, 2026

DOI: https://doi.org/10.21203/rs.3.rs-9841340/v1

License: This work is licensed under a Creative Commons Attribution 4.0 International License.
Read Full License

Additional Declarations: No competing interests reported.

Development of Forest Fire Hotspot Identification and Rapid Evaluation Technique for Tropical Landscapes Utilizing Open-access Climatic and Soil Data (FIRE-TROPICS)

Geronimo Allan Jerome G. Acosta[1*], John Vincent C. Colili[1], Rodolfo O. Abalus, Jr.[1], Jean V. Malolos[2]

[1]Department of Environmental Science, Palawan State University, Tiniguiban Heights, Puerto Princesa City, 5300, Philippines.
[2]Department of Computer Science, University of the Philippines Diliman, Diliman, Quezon City, 1101, Metro Manila, Philippines.

*Corresponding author(s). E-mail(s): gacosta@psu.palawan.edu.ph;

Abstract

Climate change is increasing fire risk in tropical forests traditionally considered fire-resilient, as demonstrated by recent fire events within Cleopatra's Needle Critical Habitat (CNCH), Palawan. This study developed the FIRE-TROPICS framework, a rapid and scalable forest fire susceptibility mapping system integrating open-access climatic, topographic, vegetation, moisture, wind, and anthropogenic datasets within machine learning and geospatial workflows. Logistic Regression (LR) and Random Forest (RF) models were implemented to identify dominant fire predictors and generate spatial susceptibility maps. Correlation analysis revealed four major environmental clusters linking elevation, temperature, wind, vegetation-moisture indices, and anthropogenic accessibility variables. Multicollinearity analysis reduced the LR model to five independent predictors: elevation, aspect eastness, aspect northness, slope, and logarithm of distance to roads. The LR model identified elevation as the strongest predictor ($\boldsymbol{\beta = -2.14}$), indicating greater fire susceptibility at lower elevations. In the RF model, land surface temperature (0.21), elevation (0.14), and NDWI (0.12) emerged as the most important predictors, while anthropogenic variables such as distance to roads (0.04) and structures (0.03) showed weaker influence. Both models consistently identified temperature-, elevation-, and wind-related variables as dominant controls on fire occurrence. Susceptibility maps highlighted similar hotspot regions, with RF producing sharper localized hotspots and LR

generating smoother susceptibility gradients. The framework demonstrates the value of integrating machine learning and geospatial systems for rapid wildfire hotspot identification and decision support in tropical conservation landscapes facing increasing climate-driven fire risk.

Keywords: forest fire susceptibility, machine learning, geospatial analysis, remote sensing

1 Introduction

Climate change is dramatically reshaping global environmental dynamics—altering temperature regimes, disrupting precipitation patterns, and intensifying weather extremes (Intergovernmental Panel on Climate Change, 2022). These shifts give rise to novel environmental threats in regions where such hazards were once uncommon, undermining ecological equilibrium and increasing the vulnerability of human and natural systems (Diffenbaugh & Burke, 2019). In many tropical landscapes—historically characterized by humid climates and lush vegetation—the combined effects of extended dry spells, diminished soil moisture, and erratic rainfall create unprecedented ecological stress (Malhi et al., 2008). As a direct consequence, the risk of forest fires—a hazard once considered rare or localized in tropical regions—is now being exacerbated by the warming climate and shifting environmental conditions (Cochrane, 2003).

Emerging research underscores this growing concern. The latest findings from the Intergovernmental Panel on Climate Change (IPCC) indicate that rising temperatures and prolonged droughts are elevating fire risk in tropical and peatland ecosystems across Southeast Asia and the Amazon, even outside classic El Niño years; fire-induced tree mortality has also increased notably in recent decades (Intergovernmental Panel on Climate Change, 2022). In Borneo, the convergence of deforestation, peatland drainage, and drier climates has led to significant spikes in fire frequency and intensity, notably during El Niño-associated droughts (Davies-Barnard, Catto, Harper, Imron, & van Veen, 2023). Studies in Bolivia's Chiquitania region reveal that extreme dry conditions alone doubled high fire-risk areas, indicating how severe drought alone can drive fire expansion in tropical forests (Devisscher, Anderson, Aragão, Galván, & Malhi, 2016). Across Amazonia, accumulated forest loss has altered hydrological cycles—reducing moisture recycling and increasing drought severity—further elevating fire susceptibility across broad swathes of the basin (Xu et al., 2020). More broadly, global modeling shows that tropical ecoregions are seeing a more than fourfold increase in the likelihood of extreme fire-weather events today compared to pre-industrial climate baselines (Abatzoglou et al., 2025).

These global and regional patterns underscore that even relatively intact forests are increasingly exposed to fire risk. Localized in the study area, this concern is reflected in Cleopatra's Needle Critical Habitat (CNCH), where 17 fire occurrences were detected using VIIRS in March 2024. This satellite evidence is further corroborated by community-level reports on social media, including live footage of fire outbreaks in barangays straddling the CNCH boundary. Together, these observations

suggest that CNCH is not immune to the global trajectory of intensifying fire regimes and may be entering a period of heightened vulnerability.

Despite these emerging threats, there is a significant data gap: fire hazard information remains sparse in regions where fire has only recently become a concern. The novelty of fire risk in many tropical areas means that long-term records, monitoring systems, and localized models are underdeveloped, leading to critical blind spots in both hazard assessment and preparedness.

This gap underscores the urgency and relevance of the Development of Forest Fire Hotspot Identification and Rapid Evaluation Technique for Tropical Landscapes Utilizing Open-access Climatic and Soil Data (FIRE-TROPICS) project. By leveraging freely available climatic and soil datasets, FIRE-TROPICS aims to pioneer a cost-effective, scalable methodology for pinpointing emerging fire-prone areas and swiftly assessing their vulnerability—filling a crucial knowledge void and supporting proactive fire prevention in vulnerable tropical regions.

2 Materials and Methods

2.1 Study Area

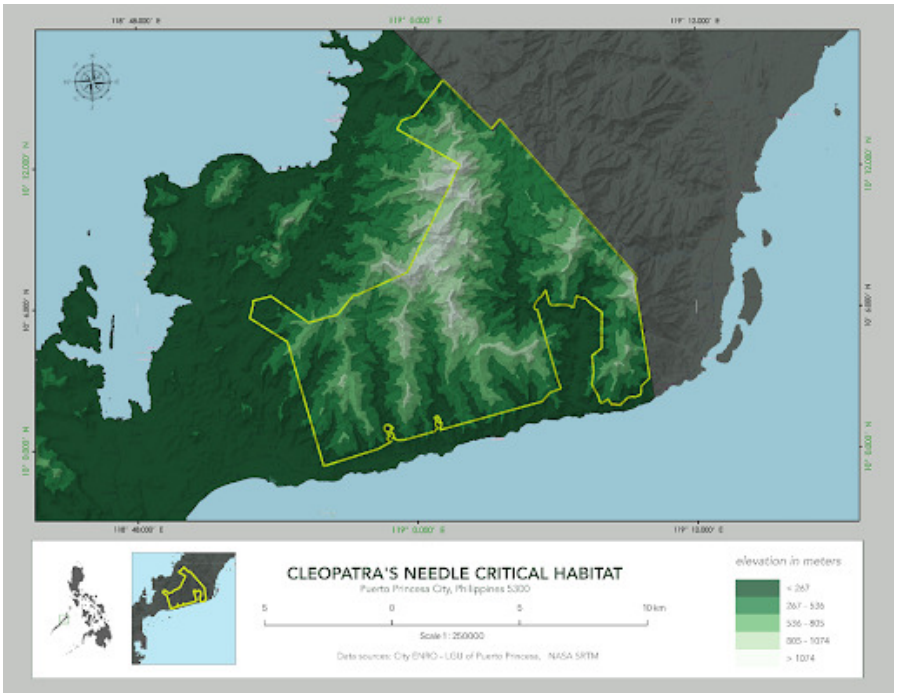


Fig. 1 A topographic map of CNCH.

The study was conducted in the CNCH, located in Puerto Princesa City, Palawan, Philippines. Covering approximately 41,350 hectares, CNCH is one of the largest and most ecologically significant forest landscapes in the country.

It was officially declared a Critical Habitat in 2017 under the Philippine Wildlife Resources Conservation and Protection Act (Republic Act 9147), recognizing its high biodiversity value and importance for long-term ecological sustainability.

CNCH is dominated by lowland dipterocarp forests, montane forests, and limestone karst ecosystems, which serve as habitat for numerous endemic and threatened species of flora and fauna. It is also a vital watershed area, providing freshwater resources to surrounding communities and contributing to the ecological stability of Puerto Princesa City. The area is home to the indigenous Batak and Tagbanua peoples, who rely on its natural resources for sustenance and cultural practices.

The topography of CNCH is characterized by rugged mountains, rolling terrain, and steep slopes, with Mount Cleopatra's Needle rising as the highest peak at 1,593 meters above sea level. The region has a tropical climate with distinct wet and dry seasons, conditions that influence vegetation cover, soil moisture, and susceptibility to forest fires. While fire occurrence in CNCH has historically been low, increasing climatic variability and human activities, such as road development and encroachment, have heightened the potential risks.

Given its ecological, cultural, and hydrological significance, CNCH provides an ideal site for developing and testing a forest fire hotspot identification and evaluation technique. Protecting this landscape is critical not only for biodiversity conservation but also for safeguarding the livelihoods of local communities and ensuring the resilience of ecosystem services in Palawan.

2.2 Data Utilized

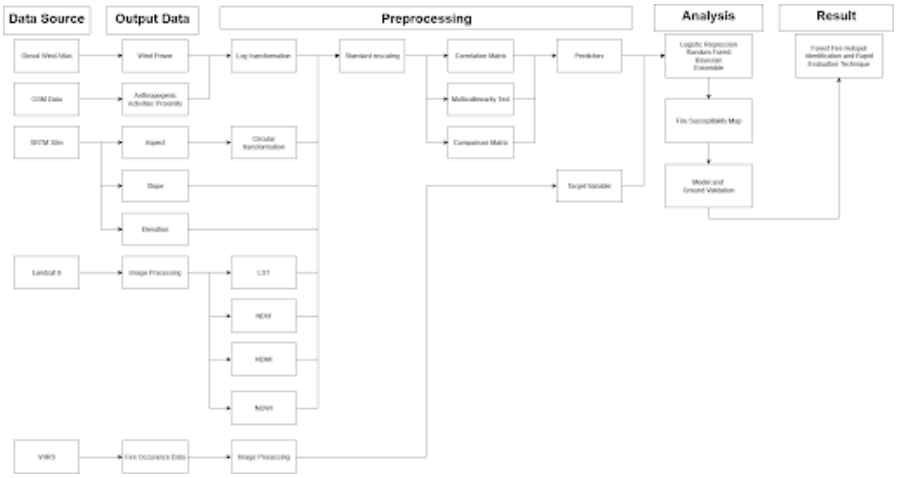


Fig. 2 The study flowchart.

This study utilized open-access datasets from reputable global repositories to ensure a cost-effective and scalable approach for identifying forest fire hotspots in the CNCH. Selected datasets represent four major categories: climate, vegetation, topography, and anthropogenic factors, which have been widely recognized as significant drivers influencing fire occurrence and spread within forested landscapes.

Climate-related variables include mean wind power and mean wind speed obtained from the Global Wind Atlas. Land Surface Temperature (LST) was derived from Landsat 9 imagery accessed through the United States Geological Survey (USGS) Earth Explorer platform.

Vegetation-related information was also generated from Landsat 9 imagery. Several spectral indices were calculated, including the Normalized Difference Moisture Index (NDMI), the Normalized Difference Vegetation Index (NDVI), and the Normalized Difference Water Index (NDWI).

Topographic variables such as elevation, slope, and aspect were obtained from the Shuttle Radar Topography Mission (SRTM) 30-meter resolution dataset through the NASA Land Processes Distributed Active Archive Center (LP DAAC).

To represent anthropogenic influences, spatial information on roads and man-made structures was collected from OpenStreetMap (OSM). Human-related features are incorporated because proximity to anthropogenic activities often increases the likelihood of fire ignition and associated disturbances.

By integrating these environmental and anthropogenic datasets, the study establishes a comprehensive framework for systematically identifying and mapping forest fire hotspots within the study area.

2.3 Fire Susceptibility Map

2.3.1 Data Pre-processing

The current study utilized 17 fire occurrences at the CNCH in the month of March, 2024. In light of the tiny sample size, the researchers employed several models to construct the susceptibility map, including logistic regression, random forest, Bayesian model, and an ensemble of the three models. To improve the accuracy, expert knowledge and ground validation was used to supplement each model whenever possible. The target variable for this study is the fire occurrence considered as a categorical variable with values of 1 and 0. The predictors are the environmental variables categorized into the following factors: topographical, vegetation/fuel, climatic, and anthropogenic.

Table 1 Environmental variables categorized into different factor groups

Environmental Factors	**Predictors**
Topographical	Elevation, Slope, Aspect
Vegetation	NDVI, NDMI, NDWI
Climatic	LST, Wind Speed, Wind Power
Anthropogenic	Distance from roads (DFR), Distance from structures (DFS)

Circular variables such as aspect were converted to continuous values using the sine and cosine functions. Additionally, skewed variables such as wind power, distance from roads (DFR), and distance from structures (DFS) were transformed using the logarithm function and the predictors were re-scaled using their z-scores before fitting into each model.

The logarithmic transformation used was,

$$x' = \log(x + c) \tag{1}$$

where x' is the transformed value, x is the raw value, and c is a small constant (1 in the present study).

The z-scores of each predictors were calculated using the following equation,

$$z = \frac{x - \mu}{\sigma} \tag{2}$$

where z is the rescaled value (z-score), x is the initial value, μ is the mean of the predictor, and σ is the standard deviation of the predictor.

The correlation matrix of the predictors was first examined to identify and either combine or remove highly correlated variables. Decisions on variable removal were guided not only by the statistical results but also by expert judgment regarding the relative importance of each predictor. After this step, a multicollinearity test using the Variance Inflation Factor (VIF) was conducted to further eliminate variables that exhibited strong dependence on others. A threshold of VIF < 10.0 was adopted to indicate acceptable levels of collinearity. The procedure was carried out iteratively, with the variable showing the highest VIF dropped in each round until all remaining predictors satisfied the criterion.

The target variable, fire occurrences, only has 17 data points. Negative samples were randomly selected from the area and assigned with the value of 0.

2.3.2 Correlation matrix

Linear-Linear Correlation

The Pearson correlation coefficient was used to calculate the pair-wise correlation between two linear variables X and Y,

$$r_{X,Y} = \frac{n \sum x_i y_i - (\sum x_i)(\sum y_i)}{\sqrt{\left[n \sum x_i^2 - (\sum x_i)^2\right]\left[n \sum y_i^2 - (\sum y_i)^2\right]}} \tag{3}$$

Where,

$$\begin{aligned} r_{X,Y} &= \text{Pearson correlation coefficient between variables } X \text{ and } Y \\ n &= \text{number of samples} \\ x_i &= \text{ith sample in } X \\ y_i &= \text{ith sample in } Y \end{aligned}$$

Circular-Linear Correlation

Circular Statistics was used to calculate the pair-wise correlation between a linear variable X and a circular variable θ,

$$r_{X,\theta} = \sqrt{\frac{r_{X,\sin\theta}^2 + r_{X,\cos\theta}^2 - 2r_{X,\sin\theta}r_{X,\cos\theta}r_{\sin\theta,\cos\theta}}{1 - r_{\sin\theta,\cos\theta}^2}} \tag{4}$$

Where,

$$\begin{aligned} r_{X,\theta} &= \text{correlation coefficient between variables } X \text{ and } \theta \\ r_{X,\sin\theta} &= \text{Pearson correlation coefficient between variables } X \text{ and } \sin\theta \\ r_{X,\cos\theta} &= \text{Pearson correlation coefficient between variables } X \text{ and } \cos\theta \\ r_{\sin\theta,\cos\theta} &= \text{Pearson correlation coefficient between variables } \sin\theta \text{ and } \cos\theta \end{aligned}$$

Circular-Circular Correlation

Circular Statistics was used to calculate the pair-wise correlation between two circular variables θ_1 and θ_2,

$$r_{\theta_1,\theta_2} = \frac{\sum_{i=1}^{n} \sin(\theta_{1i} - \bar{\theta}_1)\sin(\theta_{2i} - \bar{\theta}_2)}{\sqrt{\sum_{i=1}^{n} \sin^2(\theta_{1i} - \bar{\theta}_1) \sum_{i=1}^{n} \sin^2(\theta_{2i} - \bar{\theta}_2)}} \tag{5}$$

Where,

$$\begin{aligned} r_{\theta_1,\theta_2} &= \text{correlation coefficient between variables } \theta_1 \text{ and } \theta_2 \\ n &= \text{number of samples} \\ \theta_{1i} &= \text{ith sample in } \theta_1 \\ \theta_{2i} &= \text{ith sample in } \theta_2 \\ \bar{\theta}_1 &= \text{mean of } \theta_1 \\ \bar{\theta}_2 &= \text{mean of } \theta_2 \end{aligned}$$

2.3.3 Multicollinearity Test using Variance Inflation Factor (VIF)

Multicollinearity occurs when predictor variables in a regression model are highly correlated, making it difficult to isolate their individual effects on the dependent variable. To assess multicollinearity, the VIF is commonly used. VIF measures how much the variance of a regression coefficient is inflated due to correlation with other predictors.

The VIF for the i-th predictor was computed as:

$$\text{VIF}_i = \frac{1}{1 - R_i^2} \tag{6}$$

where R_i^2 is the coefficient of determination obtained by regressing the i-th predictor against all other predictors in the model. A threshold of VIF < 10 was used in this study.

2.3.4 Logistic Regression

Logistic regression models the probability that a binary outcome Y (here: fire = 1 vs non-fire = 0) occurs given a set of predictors X. It is appropriate for fire-susceptibility mapping because it directly estimates probability and produces interpretable coefficients.

Given a set of predictors $X = \{X_i\}$, a linear regression model is generated as follows,

$$z = \beta_0 + \beta_1 X_1 + \beta_2 X_2 + \beta_3 X_3 + \cdots + \beta_N X_N \tag{7}$$

The probability of fire occurrence was then estimated using the logistic function:

$$P(\text{fire} = 1 \mid X) = \frac{1}{1 + e^{-z}} \tag{8}$$

The parameters β_i are log-odds change per unit increase in X_i, holding others constant and N is the total number of predictors. This probability value, ranging between 0 and 1, represents the likelihood of fire occurrence at that pixel. By calculating probabilities for all pixels, a continuous fire susceptibility surface is produced.

2.3.5 Random Forest

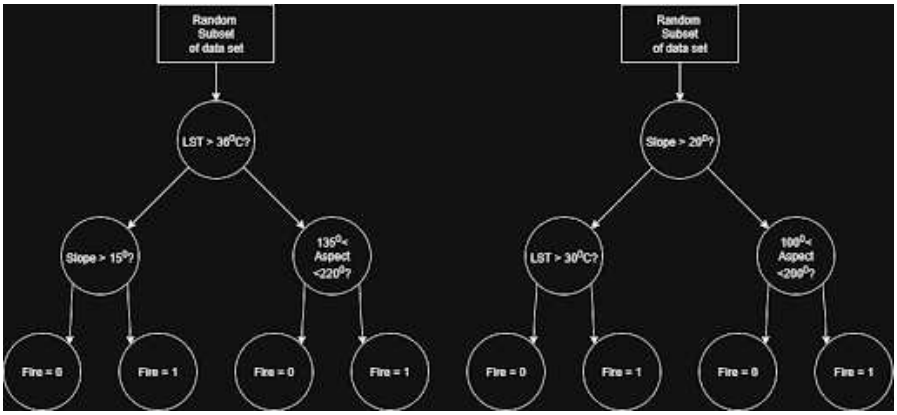


Fig. 3 Sample random forest showing the features and leaves of two trees.

Random forest is an ensemble learning method that builds a large number of decision trees and combines their results to improve predictive accuracy and stability. Each tree is trained on a bootstrap sample of the data, and at each split, only a random subset of predictors is considered (Fig. 3). This dual randomization (sampling both data and predictors) reduces correlation between trees and enhances generalization performance.

After training the random forest model, it can be applied to generate a spatial fire susceptibility map. For each pixel in the study area, the predictor values are used as input to the ensemble of decision trees. Each tree in the forest produces a classification

(fire or non-fire), and the final probability of fire occurrence is obtained by averaging the predictions across all trees:

$$P(\text{fire} = 1 \mid X) = \frac{1}{T} \sum_{t=1}^{T} h_t(X) \tag{9}$$

where T is the total number of trees and $h_t(X)$ is the prediction of the t-th tree. The output is a probability surface ranging from 0 to 1, representing the likelihood of fire occurrence at each pixel.

2.4 Software Architecture

The Forest Fire Model Mapping Dashboard was developed using a client-server web application architecture designed to support geospatial raster processing, machine learning-based prediction, and interactive visualization of forest fire susceptibility maps (Fig. 4). The system integrates a Flutter Web frontend with a FastAPI backend, enabling efficient communication between the user interface and the prediction engine through RESTful API requests. The frontend allows users to upload raster datasets, select prediction models, execute analyses, and visualize generated susceptibility outputs, while the backend handles prediction processing, raster management, and output generation through a modular architecture deployed using the Uvicorn ASGI server.

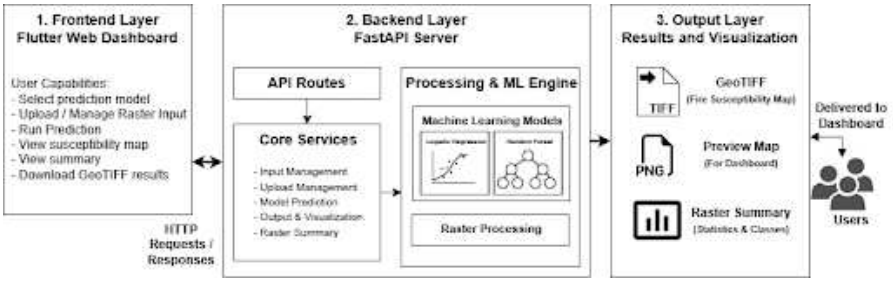


Fig. 4 Overall Software Architecture of the Forest Fire Model Mapping Dashboard.

3 Results and Discussions

3.1 Correlation Matrix

This study considered eleven environmental parameters summarized in Table 1. The multiple correlation matrix presented in Fig. 5 was generated through pairwise correlation analysis among the eleven environmental variables to examine relationships and potential dependencies among predictors. The analysis revealed four distinct patterns or clusters of relationships among the variables, indicating varying levels of association between environmental factors within the study area.

The first cluster consisted of elevation, LST, logarithm of wind power, and logarithm of wind speed, which exhibited strong correlations ranging from 50–98%. This

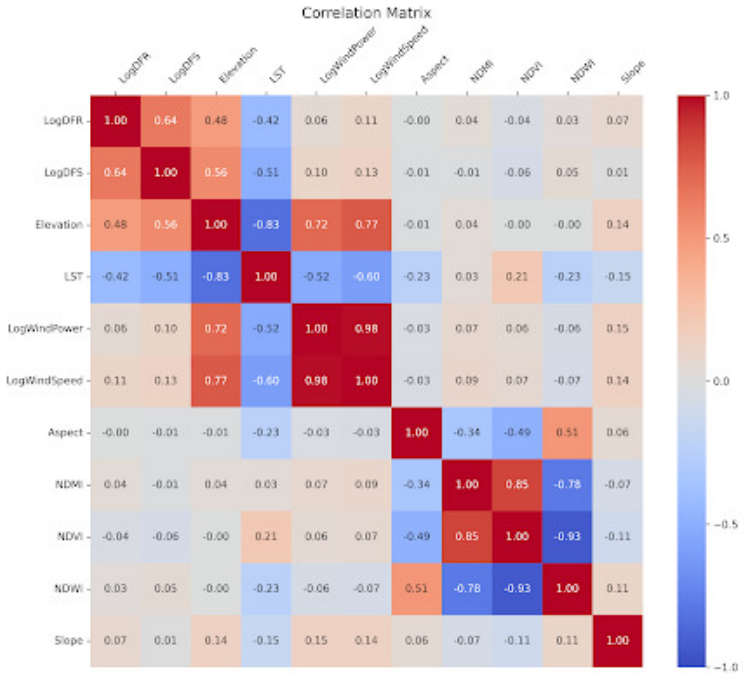


Fig. 5 Correlation matrix of environmental variables, using linear–linear, linear–circular, or circular–circular measures as appropriate.

pattern is consistent with established atmospheric processes, as wind speed and wind energy are influenced by both elevation and temperature conditions. Wind formation is driven by atmospheric pressure gradients resulting from uneven heating of the Earth's surface due to continuous solar energy input (Brower & Bailey, 2012; Kumar & Dayal, 2026). Variations in elevation may therefore affect thermal conditions and consequently influence wind-related parameters across the study area.

The second cluster involved aspect and the surface indices, specifically the NDMI, NDVI, and NDWI, which showed moderate to strong correlations ranging from 30–93%. These relationships suggest that terrain orientation influences moisture, vegetation, and water distribution patterns within the CNCH. Similar aspect-dependent relationships have also been reported in other landscapes, indicating that such patterns are commonly associated with topographic controls on environmental conditions rather than being unique to CNCH (Xiong & Wang, 2022; Zhan, Liu, Li, Wu, & Zhong, 2012).

The third cluster was characterized by the relationship between the LogDFR and the LogDFS, which showed a positive correlation of 64%. This result is expected because roads are commonly linked with settlement expansion and other forms of human-built infrastructure. Road networks often facilitate access and development,

resulting in the spatial association between transportation systems and structures (Alexander et al., 1977; Lagesse, Bordin, & Douady, 2019; Song, Du, & Wang, 2024).

The fourth pattern involved slope, which showed no significant correlation with other environmental predictors. This finding was somewhat unexpected because slope is generally assumed to influence or vary alongside several environmental factors. For example, land surface temperature may vary considerably across areas with steep slopes and heterogeneous land cover (Maeda, 2014). However, the observed pattern may represent characteristics of tropical environments or conditions specific to CNCH (Gallardo-Cruz, Pérez-García, & Meave, 2009). Previous studies suggest that weak or absent relationships between slope and environmental variables may be attributed to the scale-dependent and context-specific nature of topographic controls in tropical landscapes, where environmental conditions are often influenced more strongly by elevation, aspect, climate, and anthropogenic factors than by slope alone (Gallardo-Cruz et al., 2009; Xiong & Wang, 2022). Nevertheless, the primary purpose of this analysis was to establish the relative independence of slope as a predictor variable rather than to investigate the mechanisms responsible for its observed behavior.

3.2 Logistic Regression

Based on the exploratory analysis using the correlation matrix, several predictors exhibited strong correlations with one another. Because logistic regression is sensitive to interdependence among predictor variables, it is necessary to reduce the predictor set to a subset of relatively independent variables (Kutner, Nachtsheim, Neter, & Li, 2005; Menard, 2002). Although this may be achieved by selecting a representative variable from each previously identified cluster, a more rigorous approach is to conduct a multicollinearity analysis using VIF and iteratively eliminate predictors until an acceptable set of variables is obtained.

3.2.1 Multicollinearity Test using Variance Inflation Factor

Table 2 summarizes the results of the iterative VIF analysis conducted to identify an acceptable set of predictors. Aspect was represented as two independent variables corresponding to its eastness (sine aspect) and northness (cosine aspect). In each iteration, the predictor with the highest VIF value was removed. This process was repeated until all remaining predictors exhibited VIF values of 10 or below (Hair, Black, Babin, & Anderson, 2019).

The final set of predictors consisted of elevation, Aspect_sin (eastness), Aspect_cos (northness), logarithm of distance to roads (LogDFR), and slope. Aspect was represented through its sine and cosine transformations to capture its directional characteristics more effectively. Specifically, Aspect_sin represents the east–west orientation component (eastness), while Aspect_cos represents the north–south orientation component (northness). This transformation avoids issues associated with the circular nature of aspect data and allows directional effects to be incorporated more appropriately into subsequent analyses.

It is important to note that the final predictor set could also be interpreted as a representative selection from the previously identified clusters of correlated variables.

Table 2 VIF results for environmental variables, showing multiple recursions applied until all retained variables met the threshold of 10

Variable	VIF1	VIF2	VIF3	VIF4	VIF5	VIF6	VIF7	VIF8
Aspect_sin	1.50	1.49	1.45	1.15	1.15	1.09	1.09	1.01
Aspect_cos	1.17	1.17	1.16	1.12	1.12	1.12	1.12	1.06
LogDFR	21.92	21.78	21.63	21.54	19.91	19.70	13.19	8.90
LogDFS	28.26	26.94	26.90	26.83	21.93	21.88		
Elevation	39.20	31.76	31.55	30.81	13.18	7.76	6.60	6.58
LST	245.46	193.82	186.64	129.37				
NDMI	151.53	150.90	106.18	45.55	35.92	14.52	13.21	
NDVI	586.36	586.34						
NDWI	472.02	471.80	226.52					
Slope	7.68	7.68	7.67	7.66	7.47	6.85	6.84	5.20
LogWindPower	823.06	118.25	117.83	117.52	47.58			
LogWindSpeed	1332.95							

Elevation was selected from Cluster 1, aspect from Cluster 2, which was subsequently decomposed into its eastness and northness components, and LogDFR from Cluster 3. Slope was retained from Cluster 4, where it remained as the only independent variable due to its lack of significant correlation with the other predictors. This selection approach reduced redundancy among variables while preserving key environmental characteristics relevant to the analysis.

3.2.2 Logistic Regression Model

Using the final set of five (5) predictors

$$X = \{\text{Elevation}, \text{Aspect_sin}, \text{Aspect_cos}, \text{LogDFR}, \text{Slope}\} \tag{10}$$

a logistic regression model was constructed following the linear predictor:

$$z = \beta_0 + \beta_1 X_1 + \beta_2 X_2 + \beta_3 X_3 + \beta_4 X_4 + \beta_5 X_5 \tag{11}$$

The probability of fire occurrence was then estimated using the logistic function:

$$P(\text{fire} = 1 \mid X) = \frac{1}{1 - e^{-z}} \tag{12}$$

Table 3 summarizes the estimated values of the regression coefficients β_i. The magnitudes and signs of the regression coefficients indicate the relative influence and direction of each predictor on the probability of fire occurrence. The results identified elevation as the most influential predictor ($\beta_1 = -2.14$), with the negative coefficient indicating an inverse relationship with fire occurrence probability. This suggests that fire occurrence is more likely at lower elevations. Because elevation is strongly correlated with the predictors belonging to Cluster 1, its relationship with fire occurrence also reflects the influence of other environmental variables. Elevation exhibited positive correlations with the logarithm of wind speed and logarithm of wind power, implying that lower elevations are generally associated with lower wind speeds and lower wind power, conditions under which fire occurrence was more likely in the study area. Conversely, elevation was negatively correlated with LST, indicating that lower

elevations are generally associated with higher temperatures, which may contribute to increased fire occurrence probability. Similar relationships between elevation and wildfire activity have been reported in previous studies, where elevation influences local temperature, fuel dryness, and atmospheric conditions associated with fire danger (Alizadeh, Abatzoglou, Adamowski, et al., 2023; Bera et al., 2025).

Table 3 Estimated logistic regression coefficients and VIF values for environmental predictors of forest fire occurrence

Predictor	Coefficient	VIF
Intercept	$\beta_0 = -1.52$	
Elevation	$\beta_1 = -2.14$	6.58
Aspect_sin	$\beta_2 = -0.40$	1.01
Aspect_cos	$\beta_3 = -0.06$	1.06
Slope	$\beta_4 = 0.29$	5.20
LogDFR	$\beta_5 = 0.09$	8.90

Aspect_sin ($\beta_2 = -0.40$) and Aspect_cos ($\beta_3 = -0.06$) describe the directional influence of terrain orientation on fire occurrence probability. The negative coefficient of Aspect_sin indicates that increasing eastness reduces the likelihood of fire occurrence, implying that west-facing slopes are relatively more susceptible to fire occurrence. This finding agrees with previous studies showing that west-facing terrain often receives greater solar radiation during hotter periods of the day, resulting in warmer and drier surface conditions that enhance fire susceptibility (Oregon State University Extension, 2023). In contrast, the relatively small coefficient of Aspect_cos suggests that terrain northness or southness had only a limited influence on fire occurrence probability. Since aspect was strongly correlated with NDVI, NDMI, and NDWI in Cluster 2, these results further imply that vegetation cover, surface moisture, and water distribution may indirectly influence fire occurrence through their association with terrain orientation (Chew, Ooi, Pang, & Lim, 2026; Gupta, Shukla, & Shukla, 2025; Lee, Ahn, & Im, 2026).

Slope ($\beta_4 = 0.29$) exhibited a moderate positive relationship with fire occurrence probability, suggesting that steeper terrain is generally more prone to fire occurrence. This finding agrees with the results of (Lee et al., 2026), which may be attributed to the easier propagation of fire on steeper slopes (Taylor, Collins, Fedrigo, & Lindenmayer, 2025). On the other hand, the opposite relationship was reported by (Chen et al., 2025). However, their findings may have been influenced by the strong negative correlation between slope and wind speed observed in their study, wherein lower slopes experienced higher wind speeds, potentially resulting in a higher probability of fire occurrence.

The logarithm of distance to roads (LogDFR) ($\beta_5 = 0.09$) showed only a weak positive relationship with fire occurrence probability. Consequently, because LogDFR was positively correlated with the logarithm of distance to structures (LogDFS) in Cluster 3, this result also suggests that proximity to human-built infrastructure was

not a major determinant of fire occurrence probability in CNCH. This contradicts several studies reporting that anthropogenic variables and road metrics amplify wildfire occurrence (Ciesielski et al., 2022; Jaafari, Rahmati, Zenner, & Mafi-Gholami, 2022; Milanović et al., 2023). However, similar findings were reported by Mostafa et al. (2024 and 2025), who showed that road density and road-link metrics alone do not consistently explain wildfire occurrence and that their effects vary spatially depending on local environmental conditions. Likewise, (Narayanaraj & Wimberly, 2012) observed only a weak relationship between proximity to roads and lightning-caused fires, suggesting that anthropogenic accessibility may not always be a dominant wildfire driver. In the case of CNCH, environmental and topographic controls may have exerted stronger influence on fire occurrence probability than anthropogenic accessibility factors.

3.3 Random Forest

The Random Forest model was implemented in Python with eleven (11) input predictors consisted of raster datasets representing aspect, LogDFR, LogDFS, elevation, LST, NDMI, NDVI, NDWI, slope, LogWindPower, and LogWindSpeed. Fire occurrence points were imported from an Excel file, converted into a geospatial point dataset using their longitude and latitude coordinates, and reprojected to match the coordinate reference system of the raster predictors. Raster values were then extracted at each fire occurrence point to create the positive training samples, which were assigned a fire class value of 1.

To represent non-fire locations, 500 random pixels were sampled from the raster extent and assigned a fire class value of 0. Predictor values were extracted from the same set of raster layers at these random locations. The positive fire samples and negative random samples were then combined into a single training dataset. The Random Forest classifier was trained using these predictors as explanatory variables and the binary fire/non-fire class as the response variable. In this implementation, the model used 200 decision trees and a fixed random state of 42 to ensure reproducibility. Random Forest has been widely applied in wildfire susceptibility and occurrence modeling because of its ability to capture nonlinear interactions among environmental and anthropogenic predictors while maintaining strong predictive performance (Bera et al., 2025; Gupta et al., 2025; Milanović et al., 2023).

Table 4 summarizes the feature importance scores generated by the Random Forest fire susceptibility model. Among all predictors, LST emerged as the most important variable with an importance score of 0.21, followed by elevation (0.14) and NDWI (0.12). Wind-related variables, namely LogWindSpeed and LogWindPower, also showed relatively high importance values of 0.10 each. In contrast, anthropogenic variables such as LogDFR (0.04) and LogDFS (0.03) exhibited the lowest importance scores.

The Random Forest results are generally consistent with the findings of the logistic regression model and the earlier correlation clustering analysis. In the logistic regression model, elevation was identified as the most influential predictor with a large negative coefficient ($\beta_1 = -2.14$), indicating that lower elevations were more susceptible to fire occurrence. The Random Forest model similarly identified elevation as

Table 4 Feature Importance Scores of Environmental Predictors in the Random Forest Fire Susceptibility Model

Predictor	Importance
LST	0.21
Elevation	0.14
NDWI	0.12
LogWindSpeed	0.10
LogWindPower	0.10
Aspect	0.09
Slope	0.07
NDMI	0.06
NDVI	0.05
LogDFR	0.04
LogDFS	0.03

one of the dominant predictors, reinforcing the importance of topographic controls on fire occurrence probability in CNCH. Elevation strongly influences local microclimatic conditions, vegetation composition, and fuel moisture dynamics, which collectively affect wildfire probability (Gupta et al., 2025; Lee et al., 2026). Lower elevations generally experience warmer and drier conditions that are more favorable for fire ignition and spread.

The importance of LST in the Random Forest model also supports the interpretations derived from Cluster 1 of the correlation analysis, where elevation, LST, LogWindSpeed, and LogWindPower formed a strongly correlated group. Because elevation was negatively correlated with LST, the high importance of LST suggests that warmer surface conditions strongly contribute to fire susceptibility. Likewise, the relatively high importance values of LogWindSpeed and LogWindPower indicate that atmospheric conditions associated with wind behavior remain significant contributors to fire occurrence. This finding agrees with previous studies showing that elevated surface temperatures enhance fuel desiccation and reduce vegetation moisture content, thereby increasing fire susceptibility (Chen et al., 2025; Taylor et al., 2025). Wind conditions further contribute to wildfire behavior by enhancing oxygen supply, accelerating fuel drying, and facilitating rapid flame propagation across landscapes (Liu, Zhang, Wang, Li, & Zhao, 2024). Strong winds may also transport embers over long distances, increasing the likelihood of secondary ignitions.

The vegetation- and moisture-related indices belonging to Cluster 2 also demonstrated moderate importance in the Random Forest model. NDWI ranked as the third most important predictor (0.12), while NDMI (0.06) and NDVI (0.05) showed comparatively smaller but still meaningful contributions. These results suggest that surface moisture availability plays a substantial role in determining fire susceptibility within the study area. Moisture-related indices such as NDWI and NDMI are commonly associated with vegetation water content and fuel dryness, both of which strongly regulate ignition probability and fire intensity (Chew et al., 2026; Gupta et al., 2025). Lower moisture availability generally corresponds to higher fire susceptibility. The moderate importance of aspect (0.09) further supports the earlier observation that

terrain orientation influences vegetation and moisture distribution across the landscape. Terrain orientation affects solar radiation exposure, evapotranspiration, and local microclimate, thereby influencing vegetation productivity and fuel moisture conditions (Mostafa, Elia, Giannico, Lafortezza, & Sanesi, 2024; Taylor et al., 2025). Slopes receiving greater solar exposure often experience drier fuel conditions that favor fire occurrence. Together, these findings indicate that topographic orientation indirectly affects fire occurrence through its relationship with vegetation cover and surface moisture conditions.

Slope exhibited a moderate importance score of 0.07, which is consistent with the logistic regression model where slope showed a positive relationship with fire occurrence probability ($\beta_4 = 0.29$). Although slope formed an independent cluster in the correlation analysis, its moderate importance in both models suggests that it contributes unique information related to terrain-driven fire spread dynamics. Steeper slopes can accelerate uphill fire spread by increasing flame preheating of upslope fuels and enhancing convective heat transfer (Lee et al., 2026; Liu et al., 2024). This mechanism commonly results in greater fire susceptibility in mountainous terrain.

Finally, the low importance scores of LogDFR and LogDFS indicate that proximity to roads and structures had comparatively limited influence on fire occurrence probability within CNCH. This result is consistent with the logistic regression model, where LogDFR also exhibited a very small coefficient ($\beta_5 = 0.09$). Although roads and structures were positively correlated within Cluster 3, their weak contribution in both models suggests that anthropogenic accessibility factors are less important than environmental and topographic controls in determining fire occurrence within the study area. Although anthropogenic variables are frequently reported as major wildfire drivers, several studies have demonstrated that their influence may vary spatially depending on local environmental conditions and ignition mechanisms (Mostafa et al., 2024; Narayanaraj & Wimberly, 2012). In relatively remote or forest-dominated systems, climatic and topographic controls may outweigh the influence of roads and built infrastructure.

Overall, the Random Forest model validates the major patterns identified in both the logistic regression analysis and the correlation clustering results. Cluster 1 variables associated with temperature, elevation, and wind emerged as the dominant controls on fire occurrence, while Cluster 2 variables related to moisture and vegetation exhibited secondary influence. In contrast, Cluster 3 anthropogenic variables contributed relatively little to fire susceptibility prediction. Meanwhile, Cluster 4, represented solely by slope, maintained moderate importance in both the Random Forest and logistic regression models despite its relative independence from the other predictors. The consistency between the Random Forest and logistic regression results suggests that the dominant environmental controls identified in the study are robust across both linear statistical and nonlinear ensemble-learning approaches (Gupta et al., 2025; Milanović et al., 2023).

3.4 Susceptibility Maps

The susceptibility maps were generated by applying the logistic regression and Random Forest models to all pixels within the boundaries of the CNCH map. The logistic

regression model outputs the probability of fire occurrence at each pixel given the values of five predictors: elevation, aspect (decomposed into eastness and northness), logarithm of the distance from roads, and slope. Logistic regression has been widely used in wildfire susceptibility studies because of its interpretability and ability to estimate probabilistic relationships between environmental predictors and fire occurrence (Milanović et al., 2023; Zhang et al., 2023). The probabilistic nature of logistic regression allows the resulting susceptibility surface to vary continuously across the landscape, producing smoother spatial transitions between low- and high-risk areas.

The Random Forest model decides whether fire occurrence is present (value of 1) or absent (value of 0) and outputs the average decision of all decision trees for each pixel given the values of eleven predictors: LST, elevation, NDWI, logarithm of wind speed, logarithm of wind power, aspect, slope, NDMI, NDVI, logarithm of distance from roads, and logarithm of distance from structures. The average decision, ranging from 0 to 1, was interpreted as the probability of fire occurrence. Random Forest models are particularly effective in wildfire susceptibility mapping because they capture nonlinear interactions and threshold-dependent relationships among predictors that are often difficult to represent using linear statistical approaches (Bera et al., 2025; Gupta et al., 2025).

The final susceptibility map is represented as a heatmap of the probability of fire occurrence for each model. Figure 6 shows the generated fire susceptibility maps for the logistic regression model (left) and Random Forest model (right). Both maps highlighted generally similar areas with high fire occurrence probability, indicating agreement between the two modeling approaches regarding the dominant spatial controls on wildfire occurrence. However, the logistic regression map exhibited smoother gradients compared to the Random Forest map. This behavior is expected because logistic regression estimates a continuous linear probability surface based on additive predictor contributions, resulting in gradual spatial transitions. In contrast, Random Forest models partition the predictor space into multiple nonlinear decision regions through recursive tree splitting, which tends to generate sharper spatial boundaries and more localized hotspots (Gupta et al., 2025; Milanović et al., 2023).

Figure 7 summarizes the distributions of fire occurrence probabilities in terms of area (hectares) covered on a logarithmic scale. A linear decrease in the logarithmic distribution would imply an exponential spatial decay of probabilities from the hotspots. The logistic regression distribution (left) exhibited a gradual decrease from 0.0 toward 0.8, suggesting a relatively smooth transition of susceptibility away from hotspot regions. On the other hand, the Random Forest distribution decreased rapidly from 0.0 to 0.8, indicating a steeper susceptibility gradient and stronger localization of high-probability regions. This result further supports the tendency of Random Forest models to emphasize discrete high-risk zones due to nonlinear threshold effects and interaction-driven classification behavior. Similar observations have been reported in wildfire susceptibility studies where ensemble machine learning methods produced more spatially concentrated susceptibility patterns than regression-based approaches (Bera et al., 2025; Gupta et al., 2025).

The hotspots may be interpreted as local maxima within the susceptibility heatmaps and can generally be categorized into point maxima, ridge maxima, or planar

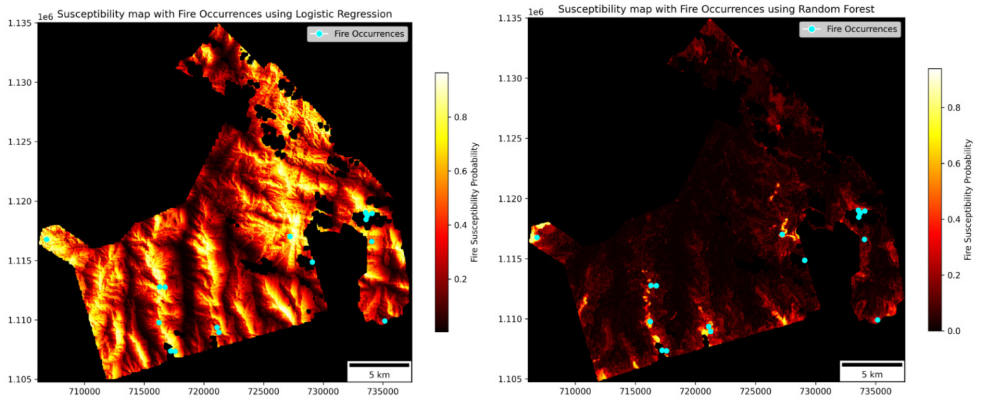


Fig. 6 Forest fire susceptibility map generated using (LEFT) logistic regression and (RIGHT) random forest. Blue points represent actual fire occurrence data

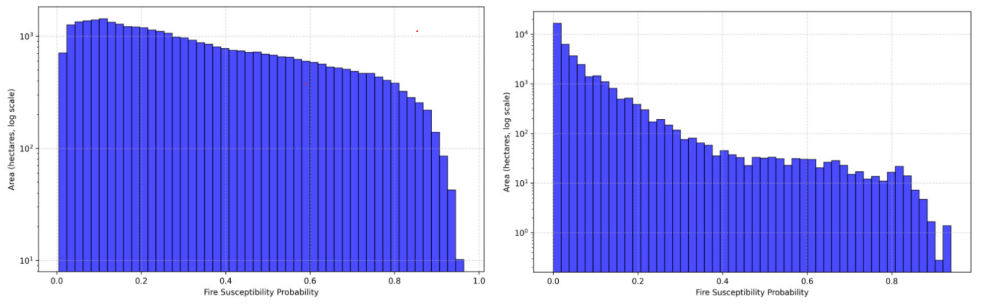


Fig. 7 Distribution of predicted probability values from the (LEFT) logistic regression model and (RIGHT) random forest model, showing the total land area (in hectares, log scale) across low- to high-susceptibility classes

maxima based on the local geometry of the susceptibility surface. In two-dimensional scalar fields, ridge-like maxima commonly emerge when a susceptibility function is strongly controlled by one or more spatial gradients that extend continuously across the landscape, such as elevation or temperature gradients. In the generated maps, the hotspots were predominantly ridge-like rather than isolated point maxima. This observation further supports the earlier finding that elevation and temperature were the dominant predictors identified by both models. Locations sharing similar elevation and temperature conditions tend to align continuously along terrain structures, thereby forming elongated susceptibility ridges across the landscape. Similar topographically controlled ridge structures have also been observed in environmental susceptibility surfaces governed primarily by terrain and climatic gradients (Lee et al., 2026; Taylor et al., 2025).

Together, these patterns suggest that Random Forest is more effective in highlighting discrete and sharply bounded hotspots, whereas logistic regression provides a more

continuous and conservative representation of landscape vulnerability. The smoother susceptibility field produced by logistic regression reflects its global linear structure, while the sharper hotspot delineation produced by Random Forest arises from its non-linear ensemble-learning framework and sensitivity to localized predictor interactions. Consequently, logistic regression may be more appropriate for identifying broad-scale susceptibility trends, whereas Random Forest may provide better localization of high-risk ignition zones for targeted management and mitigation planning (Gupta et al., 2025; Milanović et al., 2023).

3.5 Forest Fire Model Mapping Dashboard

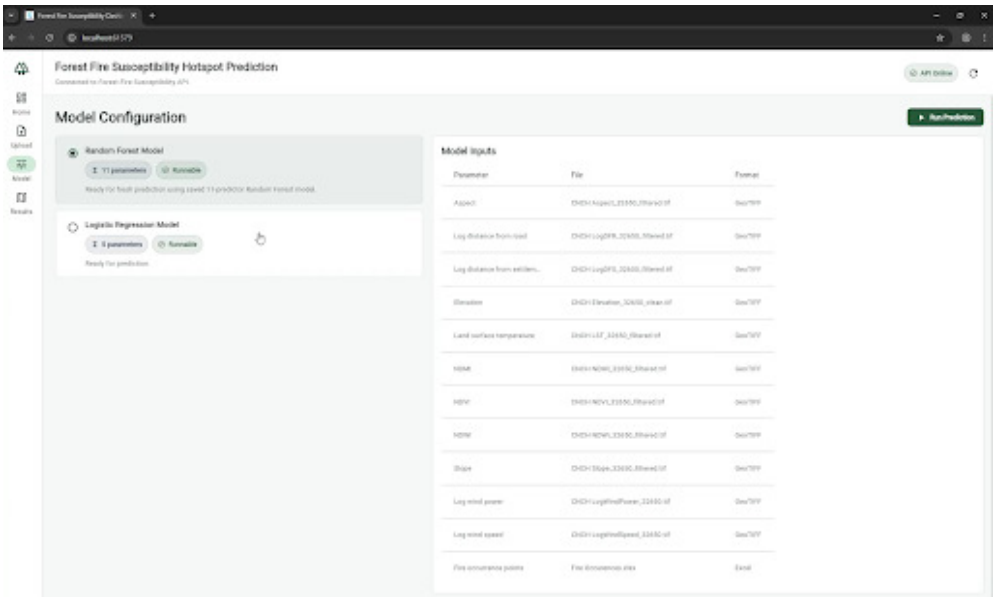


Fig. 8 Model Configuration of the Forest Fire Model Mapping Dashboard

The model configuration of the Forest Fire Model Mapping Dashboard is shown in Figure 8. Two machine learning approaches were integrated into the system: a 5-parameter Logistic Regression model and an 11-parameter Random Forest model. The dashboard was designed to provide a unified platform for preprocessing, model execution, raster generation, visualization, and statistical summarization of fire susceptibility outputs. By integrating geospatial processing and machine learning into a web-based interface, the system enables rapid spatial assessment of wildfire susceptibility across the CNCH landscape. The Logistic Regression workflow applies preprocessing operations such as feature scaling and transformation of aspect values into sine and cosine representations to capture directional characteristics before generating susceptibility probabilities. In contrast, the Random Forest model directly

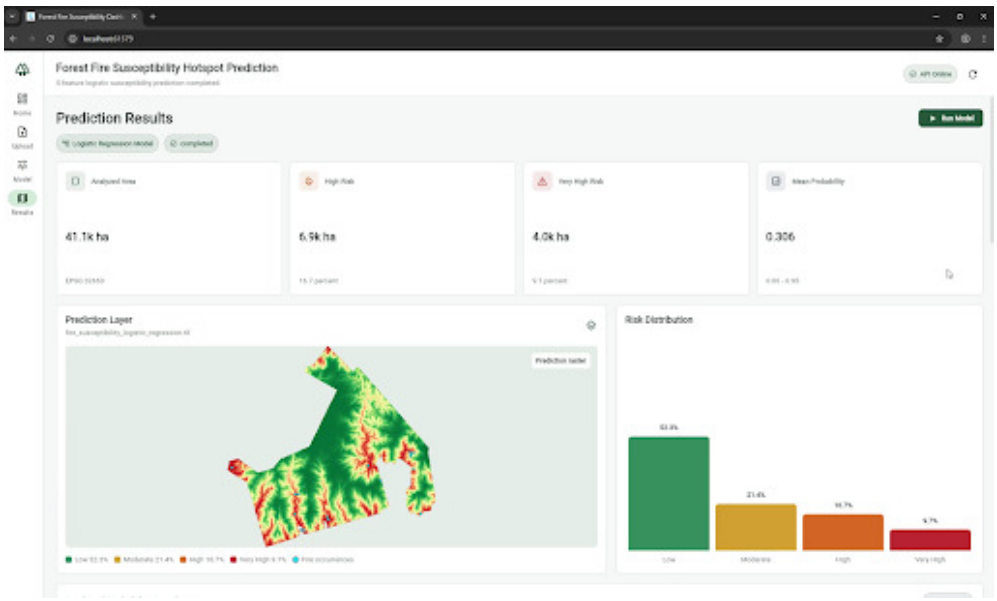


Fig. 9 Prediction Results and Raster Summary of the Forest Fire Model Mapping Dashboard

utilizes eleven raster parameters without requiring feature scaling. Both models generate raster-based susceptibility outputs using the `predict_proba()` function, enabling spatial prediction of forest fire susceptibility levels across the study area.

Figure 9 shows the prediction results and raster Summary of the Forest Fire Model Mapping Dashboard. Following prediction, the backend generates a GeoTIFF susceptibility raster and a PNG preview image for visualization within the dashboard. The actual fire occurrences are plotted in the visualization. The system also computes raster summary statistics, including total analyzed area, susceptibility category distribution, pixel counts, area coverage in hectares, and mean susceptibility values. These outputs are returned to the frontend as structured JSON responses containing downloadable raster files, preview images, and analytical summaries. Through this integrated architecture, the dashboard provides a unified decision-support platform for forest fire susceptibility analysis by combining machine learning prediction, geospatial raster processing, and web-based visualization.

4 Conclusions and Recommendations

This study developed the FIRE-TROPICS framework, an integrated machine learning and geospatial approach for forest fire susceptibility mapping within CNCH. Using open-access environmental and anthropogenic datasets, LR and RF models were implemented to identify dominant controls on fire occurrence and generate spatial susceptibility maps.

The results consistently showed that temperature, elevation, and wind-related variables are the primary drivers of forest fire occurrence within the study area. Logistic

regression identified elevation as the strongest predictor, indicating that lower elevations exhibit higher fire susceptibility. Similarly, the RF model identified LST, elevation, and NDWI as the most influential predictors. In contrast, anthropogenic accessibility variables such as distance to roads and structures exhibited comparatively weak influence, suggesting that environmental and topographic controls dominate fire occurrence patterns within CNCH.

Both susceptibility models produced generally similar hotspot regions, demonstrating agreement regarding the major spatial controls of wildfire occurrence. However, the RF model generated sharper and more localized hotspot boundaries due to its nonlinear structure, while the LR model produced smoother and more continuous susceptibility gradients. The hotspot structures predominantly appeared as ridge-like patterns aligned with elevation and temperature gradients, indicating strong terrain-driven climatic control over fire-prone zones. To operationalize the framework, a Forest Fire Model Mapping Dashboard was developed integrating machine learning prediction, geospatial raster generation, statistical summarization, and web-based visualization. The system enables rapid wildfire susceptibility assessment and provides a scalable decision-support platform for forest monitoring and management applications.

Overall, the findings demonstrate that tropical forests previously considered fire-resilient are becoming increasingly vulnerable under changing climatic conditions. The FIRE-TROPICS framework provides a practical and scalable approach for wildfire hotspot identification and spatial decision support in tropical conservation landscapes.

Acknowledgements. The authors would like to express their sincere gratitude to all individuals and institutions who contributed to the completion of this study. Special acknowledgment is extended to the Palawan State University - University Research and Creative Works Office for the internal research funding support and resources that made this work possible. We also extend our appreciation to the City Environment and Natural Resources Office (City ENRO) of Puerto Princesa for their assistance, coordination, and provision of relevant environmental information and field support during the conduct of this research. Special thanks are likewise given to all stakeholders, local experts, and partner communities who participated in consultations and shared valuable insights that contributed to the refinement and contextualization of the study framework. The authors likewise acknowledge the developers and maintainers of the open-access datasets, software platforms, and scientific resources utilized in this work, whose continued commitment to open science greatly facilitated the conduct of this research.

Declarations

Funding

This study received internal research funding support from the Palawan State University – University Research and Creative Works Office.

Conflict of interest/Competing interests

The authors declare that they have no competing interests. No financial support, personal relationships, institutional affiliations, or other circumstances exist that

could have influenced the design, conduct, analysis, interpretation, or reporting of this research.

Ethics approval and consent to participate

Not applicable.

Consent for publication

Not applicable.

Data availability

The datasets generated and/or analyzed during the current study are available from the corresponding author on reasonable request.

Materials availability

The materials utilized in this study are available from the corresponding author on reasonable request.

Code availability

The codes and scripts used in the analysis and development of the Forest Fire Model Mapping Dashboard are available from the corresponding author on reasonable request.

Author contribution

All authors contributed to the completion and finalization of this manuscript. JVCC conducted all GIS-based processing and spatial analyses for the study. GAJA performed the statistical and correlation analyses. ROA contributed to the validation of results and assisted in manuscript finalization. JVM was responsible for the development of the program module and the integration and transfer of GIS-based data into the system.

References

Abatzoglou, J.T., Kolden, C.A., Cullen, A.C., Sadegh, M., Williams, E.L., Turco, M., Jones, M.W. (2025). Climate change has increased the odds of extreme regional forest fire years globally. *Nature Communications*, *16*, 6390, https://doi.org/10.1038/s41467-025-61608-1

Alexander, C., Ishikawa, S., Silverstein, M., Jacobson, M., Fiksdahl-King, I., Angel, S. (1977). *A pattern language: Towns, buildings, construction.* Oxford University Press.

Alizadeh, M.R., Abatzoglou, J.T., Adamowski, J., et al. (2023). Elevation-dependent intensification of fire danger in the western united states. *Nature Communications*, *14*, 1773, https://doi.org/10.1038/s41467-023-37311-4

Bera, D., Raut, S., Mahata, C., Dutta, D., Datta, D., Kundu, A. (2025). Early prediction of forest fire events integrating multi-sensor datasets and machine learning techniques. *Stochastic Environmental Research and Risk Assessment*, *39*(11), 5381–5400, https://doi.org/10.1007/s00477-025-03070-5

Brower, M.C., & Bailey, B.H. (2012). *Wind resource assessment: A practical guide to developing a wind project*. Wiley.

Chen, X., Yang, Q., Chen, Z., Lei, J., Wu, T., Li, Y., Pan, X. (2025). The interaction between temperature and rainfall determines the probability of tropical forest fire occurrence in hainan island. *Frontiers in Forests and Global Change*, *8*, 1495699, https://doi.org/10.3389/ffgc.2025.1495699

Chew, Y.J., Ooi, S.Y., Pang, Y.H., Lim, Z.Y. (2026). A review of key factors influencing forest fire and wildfire susceptibility: The role of climatic, environmental, topographic, and anthropogenic variables. *Pertanika Journal of Tropical Agricultural Science*, *49*(2), 689–714,

Ciesielski, M., Bałazy, R., Borkowski, B., Szczesny, W., Zasada, M., Kaczmarowski, J., ... Milanović, S. (2022). Contribution of anthropogenic, vegetation, and topographic features to forest fire occurrence in poland. *iForest - Biogeosciences and Forestry*, *15*(4), 307–314, https://doi.org/10.3832/ifor4052-015

Cochrane, M.A. (2003). Fire science for rainforests. *Nature*, *421*(6926), 913–919, https://doi.org/10.1038/nature01437

Davies-Barnard, T., Catto, J.L., Harper, A.B., Imron, M.A., van Veen, F.J.F. (2023). Future fire risk under climate change and deforestation scenarios in tropical borneo. *Environmental Research Letters*, *18*(2), 024015, https://doi.org/10.1088/1748-9326/acb225

Devisscher, T., Anderson, L.O., Aragão, L.E.O.C., Galván, L., Malhi, Y. (2016). Increased wildfire risk driven by climate and development interactions in the bolivian chiquitania, southern amazonia. *PLOS ONE*, *11*(9), e0161323, https://doi.org/10.1371/journal.pone.0161323

Diffenbaugh, N.S., & Burke, M. (2019). Global warming has increased global economic inequality. *Proceedings of the National Academy of Sciences*, *116*(20), 9808–9813, https://doi.org/10.1073/pnas.1816020116

Gallardo-Cruz, J.A., Pérez-García, E.A., Meave, J.A. (2009). β-diversity and vegetation structure as influenced by slope aspect and altitude in a seasonally dry tropical landscape. *Landscape Ecology*, *24*(4), 473–482, https://doi.org/10.1007/s10980-009-9332-1

Gupta, P., Shukla, A.K., Shukla, D.P. (2025). Machine learning-based forest fire susceptibility mapping of southern mizoram, a part of indo-burma biodiversity hotspot. *Environmental Science and Pollution Research*, *32*, 31433–31454, https://doi.org/10.1007/s11356-025-36621-y

Hair, J.F., Black, W.C., Babin, B.J., Anderson, R.E. (2019). *Multivariate data analysis* (8th ed.). Cengage.

Intergovernmental Panel on Climate Change (2022). Tropical forests (cross-chapter paper 7). *Climate change 2022: Impacts, adaptation and vulnerability* (pp. 2313–2362). Cambridge University Press.

Jaafari, A., Rahmati, O., Zenner, E.K., Mafi-Gholami, D. (2022). Anthropogenic activities amplify wildfire occurrence in the zagros eco-region of western iran. *Natural Hazards*, *114*(1), 457–473, https://doi.org/10.1007/s11069-022-05397-6

Kumar, S.S., & Dayal, K.K. (2026). Wind resource assessment and energy modelling of smaller outer islands in fiji. *Royal Society Open Science*, *13*(3), 251714, https://doi.org/10.1098/rsos.251714

Kutner, M.H., Nachtsheim, C.J., Neter, J., Li, W. (2005). *Applied linear statistical models* (5th ed.). McGraw-Hill/Irwin.

Lagesse, C., Bordin, P., Douady, S. (2019). A graph-based approach for the structural analysis of road and building layouts. *Cartography and Geographic Information Science*, *46*(6), 526–541, https://doi.org/10.1080/15230406.2018.1559638

Lee, J., Ahn, S., Im, S. (2026). Spatial prediction of forest fire occurrence integrating human proximity: A machine learning approach for korea's eastern coast. *Forests*, *17*(2), 281, https://doi.org/10.3390/f17020281

Liu, Y., Zhang, H., Wang, S., Li, X., Zhao, F. (2024). Effects of slope and wind interaction on wildfire spread dynamics in mountainous terrain. *Fire*, *7*(6), 175, https://doi.org/10.3390/fire7060175

Maeda, E.E. (2014). Downscaling modis lst in the east african mountains using elevation gradient and land-cover information. *International Journal of Remote Sensing*, *35*(9), 3094–3108, https://doi.org/10.1080/01431161.2014.903442

Malhi, Y., Roberts, J.T., Betts, R.A., Killeen, T.J., Li, W., Nobre, C.A. (2008). Climate change, deforestation, and the fate of the amazon. *Science*, *319*(5860), 169–172, https://doi.org/10.1126/science.1146961

Menard, S. (2002). *Applied logistic regression analysis* (2nd ed.). Sage Publications.

Milanović, S., Kaczmarowski, J., Ciesielski, M., Trailović, Z., Mielcarek, M., Szczygieł, R., ... Milanović, S.D. (2023). Modeling and mapping of forest fire occurrence in the lower silesian voivodeship of poland based on machine learning methods. *Forests*, *14*(1), 46, https://doi.org/10.3390/f14010046

Mostafa, M., Elia, M., Giannico, V., Lafortezza, R., Sanesi, G. (2024). Assessing forest road network suitability in relation to the spatial occurrence of wildfires in mediterranean forest ecosystems. *Fire*, *7*(6), 175, https://doi.org/10.3390/fire7060175

Narayanaraj, G., & Wimberly, M.C. (2012). Influences of forest roads on the spatial patterns of human- and lightning-caused wildfire ignitions. *Applied Geography*, *32*(2), 878–888, https://doi.org/10.1016/j.apgeog.2011.09.004

Oregon State University Extension (2023). *The effects of topography, weather, and fuel on fire behavior.* (Pacific Northwest Extension Publication PNW 618)

Song, X., Du, L., Wang, Z. (2024). Correlation analysis of urban road network structure and spatial distribution of tourism service facilities at multi-scales based on tourists' travel preferences. *Buildings*, *14*(4), 914, https://doi.org/10.3390/buildings14040914

Taylor, C., Collins, L., Fedrigo, M., Lindenmayer, D.B. (2025). Drought, topography, and forest management shape wildfire occurrence and severity in australian montane forests. *Science of the Total Environment*, *977*, 179733, https://doi.org/10.1016/j.scitotenv.2025.179733

Xiong, Y., & Wang, H. (2022). Spatial relationships between ndvi and topographic factors at multiple scales in a watershed of the minjiang river, china. *Ecological Informatics*, *69*, 101617, https://doi.org/10.1016/j.ecoinf.2022.101617

Xu, R., Yu, P., Abramson, M.J., Johnston, F.H., Samet, J.M., Bell, M.L., ... Guo, Y. (2020). Wildfires, global climate change, and human health. *New England Journal of Medicine*, *383*(22), 2173–2181, https://doi.org/10.1056/

NEJMsr2028985

Zhan, Z.-Z., Liu, H.-B., Li, H.-M., Wu, W., Zhong, B. (2012). The relationship between ndvi and terrain factors: A case study of chongqing. *Procedia Environmental Sciences*, *12*, 765–771, https://doi.org/10.1016/j.proenv.2012.01.347

Zhang, F., Bin, Z., Luo, J., Liu, H., Qingchun, D., Wang, L., Zuo, Z. (2023). Forest fire driving factors and fire risk zoning based on an optimal parameter logistic regression model: A case study of the liangshan yi autonomous prefecture, china. *Fire*, *6*(9), 336, https://doi.org/10.3390/fire6090336